We are IntechOpen, the world's leading publisher of Open Access books Built by scientists, for scientists

6,900
Open access books available

185,000
International authors and editors

200M
Downloads

Our authors are among the

154
Countries delivered to

TOP 1%
most cited scientists

12.2%
Contributors from top 500 universities



WEB OF SCIENCE™

Selection of our books indexed in the Book Citation Index in Web of Science™ Core Collection (BKCI)

Interested in publishing with us?
Contact book.department@intechopen.com

Numbers displayed above are based on latest data collected.
For more information visit www.intechopen.com



Chapter 9

Dual-Hop Amplify-and-Forward Relay Systems with EGC over M2M Fading Channels Under LOS Conditions: Channel Statistics and System Performance Analysis

Talha Batool and Pätzold Matthias

Additional information is available at the end of the chapter

http://dx.doi.org/10.5772/55333

1. Introduction

The recently growing popularity of cooperative diversity [1–3] in wireless networks is due to its ability to mitigate the deleterious fading effects. By utilizing the existing resources of the network, a spatial diversity gain can be achieved without any extra cost resulting from the deployment of a new infrastructure. The fundamental principle of cooperative relaying is that several mobile stations in a network collaborate together to relay the transmit signal from the source mobile station to the destination mobile station. In the simplest mode of operation, the relay nodes just amplify the received signal and forward it towards the destination mobile station. They can also first decode the received signal, encode it again, and then forward it. In both cases, multiple copies of the same signal reach the destination mobile station, which can be combined to achieve a diversity gain by exploiting the virtual antenna array. In addition to the spatial diversity gain, cooperative relaying promises increased capacity, improved connectivity, and a larger coverage range [4–6].

In this paper, a dual-hop amplify-and-forward configuration has been taken into account, where there exist K mobile relays between the source mobile station and the destination mobile station. In addition, the direct link from the source mobile station to the destination mobile station is also present. Such a configuration in turn gives rise to $K+1$ diversity branches. Thus, the previously mentioned spatial diversity gain is achieved by combining the signal received from the $K+1$ diversity branches at the destination mobile station. Among the most important diversity combining techniques [7], maximal ratio combining (MRC) has been proved to be the optimum one [7]. It is widely acknowledged in the literature that a suboptimal and less complex combining technique, referred to as equal

INTECH
open science | open minds

© 2013 Batool and Matthias; licensee InTech. This is an open access article distributed under the terms of the Creative Commons Attribution License (http://creativecommons.org/licenses/by/3.0), which permits unrestricted use, distribution, and reproduction in any medium, provided the original work is properly cited.

gain combining (EGC), performs very close to MRC [7]. Studies regarding the statistical properties of EGC and MRC in non-cooperative networks over Rayleigh, Rice, and Nakagami fading channels are reported in [8–10]. Furthermore, the performance analysis of the said schemes in terms of the bit error and outage probability over Rayleigh, Rice, and Nakagami fading channels can be found in [11–13]. During the last decade, a large number of researchers devoted their efforts to analyzing the performance of cooperative networks. For example, the performance of dual-hop amplify-and-forward relay networks has been extensively investigated for different types of fading channels in [14–26]. A performance analysis in terms of the average bit error probability (BEP) as well as the outage probability of single-relay dual-hop configurations over Rayleigh and generalized-K fading channels is presented in [14] and [16], respectively. A study pertaining to the asymptotic outage behavior of amplify-and-forward dual-hop multi-relay systems with Nakagami fading channels is available in [19], whereas the diversity order is addressed in [23]. The common denominator in the works [15, 17–24] is that they consider MRC at the destination mobile station, where the authors of [24] have also included in their analysis results when EGC is deployed. Performance related issues in multi-relay dual-hop non-regenerative relay systems with EGC over Nakagami-m channels are investigated in [25, 26].

The success story of cooperative relaying in cellular networks has motivated the wireless communications research community to explore their application possibilities in mobile-to-mobile (M2M) communication systems. Relay-based M2M communication systems find their application in intervehicular systems or in other words vehicle-to-vehicle systems. Spreading the information of any kind of emergency situation on roads can be made possible with the use of relay-based M2M systems. The development of relay-based M2M communication systems, however, requires the knowledge of the propagation channel characteristics. It is well known that the multipath propagation channel can efficiently be described with the help of proper statistical models. For example, the Rayleigh distribution is considered to be a suitable distribution to model the fading channel under non-line-of-sight (NLOS) propagation conditions in classical cellular networks [27–29]; a Suzuki process represents a reasonable model for land mobile terrestrial channels [30, 31], and the generalized-K distribution is widely accepted in radar systems [32, 33]. To model fading channels under NLOS propagation conditions in relay-based M2M communication systems, the double Rayleigh distribution is the appropriate choice (see, e.g., [34, 35] and the references therein). Motivated by the applications of the double Rayleigh channel model, a generalized channel model referred to as the $N*$ Nakagami channel model has been proposed in [36]. Furthermore, an extension from the double Rayleigh channel model to the double Rice channel model that is based on the assumption of line-of-sight (LOS) propagation conditions has been proposed in [37]. The authors of [38] have explored the performance of intervehicular cooperative schemes, and they proposed optimum power allocation strategies assuming cascaded Nakagami fading. The performance of several digital modulation schemes over double Nakagami-m channels with MRC diversity has been studied in [39], whereas the BEP analysis of M-ary phase shift keying (PSK) modulated signals over double Rayleigh channels with EGC can be found in [40].

This article focuses on analyzing the statistical properties of EGC over M2M fading channels under LOS propagation conditions as well as the performance of relay-based networks in such channels. As far as the authors are aware, the statistical analysis of EGC over M2M channels assuming LOS propagation conditions has not been carried out yet. In addition,

http://dx.doi.org/10.5772/55333

the performance analysis of multi-relay dual-hop amplify-and-forward cooperative networks in such fading channels is also an open problem that calls for further work. In many practical propagation scenarios, asymmetric fading conditions can be observed in different relay links. Meaning thereby, LOS components can exist in all, none or just in some few transmission links between the source mobile station and the destination mobile station via K mobile relays. Similarly, the LOS component can be present in the direct link from the source mobile station to the destination mobile station. Thus, in order to accommodate the direct link along with the unbalanced relay links, the received signal envelope at the output of the EG combiner is modeled as a sum of a classical Rice process and K double Rice processes. Here, the classical Rice process and double Rice processes are assumed to be statistically independent. Furthermore, it is assumed that K double Rice processes are mutually independent but not necessarily identically distributed. Analytical approximations are derived for the probability density function (PDF), the cumulative distribution function (CDF), the level-crossing rate (LCR), and the average duration of fades (ADF) of the resulting sum process by exploiting the properties of a gamma process[1]. The analysis of these statistical quantities give us a complete picture of the fading channel, since the PDF can well characterize the channel's envelope distribution, and the LCR along with the ADF provide an insight into the fading behavior of the channel. Several performance evaluation measures, such as the statistics of the instantaneous signal-to-noise ratio (SNR) at the output of the equal gain (EG) combiner, amount of fading (AOF), the average BEP, and the outage probability, are thoroughly investigated in this work. It includes also a discussion on the influence of the number of diversity branches $K+1$ as well as the presence of LOS components in the transmission links on the statistics of M2M fading channels with EGC. The approximate analytical results for the PDF, CDF, LCR, ADF, the average BEP, and the outage probability are compared with those of the exact simulation results to validate the correctness of the proposed approach. From the presented results, it can be concluded that the performance of relay-based cooperative systems improves with the presence of LOS components in the relay links. In addition, if the number $K+1$ of diversity branches increases, the better is the system performance.

This article has the following structure. In Section 2, we present the system model for EGC over M2M fading channels under LOS propagation conditions in amplify-and-forward relay networks. Section 3 deals with the derivation and analysis of approximations for the PDF, CDF, LCR, and ADF of the received signal envelope at the output of the EG combiner. In Section 4, analytical approximations for the PDF as well as the moments of the SNR at the output of the EG combiner, the average BEP, and the outage probability are derived and analyzed. Section 5 studies the accuracy of the analytical approximations by simulations and presents a detailed discussion on the obtained results. Finally, the article is concluded in Section 6.

2. EGC over M2M fading channels with LOS components

In this section, we describe the system model for EGC over narrowband M2M fading channels under isotropic scattering conditions with LOS components in a dual-hop cooperative network. In the considered system, we have K mobile relays, which are connected

[1] The material in this paper was presented in part at the International Conference on Communications, ICC 2010, Cape Town, South Africa, May 2010.

in parallel between the source mobile station and the destination mobile station, as illustrated in Fig. 1. It can be seen in this figure that the direct transmission link from the source mobile station to the destination mobile station is also unobstructed.

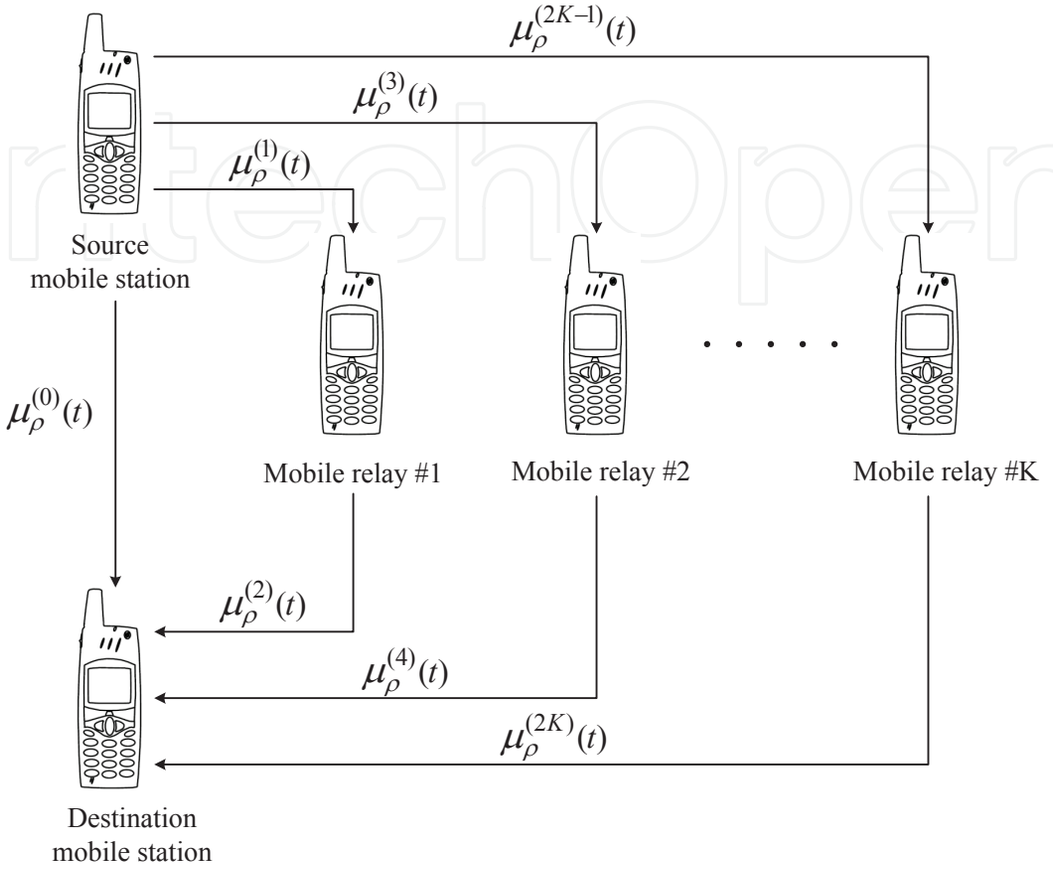


Figure 1. The propagation scenario describing K-parallel dual-hop relay M2M fading channels.

It is assumed that all mobile stations in the network, i.e., the source mobile station, the destination mobile station, and the K mobile relays do not transmit and receive a signal at the same time in the same frequency band. This can be achieved by using the time-division multiple-access (TDMA) based amplify-and-forward relay protocols proposed in [41, 42]. Thus, the signals from the $K+1$ diversity branches in different time slots can be combined at the destination mobile station using EGC.

Let us denote the signal transmitted by the source mobile station as $s(t)$. Then, the signal $r^{(0)}(t)$ received at the destination mobile station from the direct transmission link between the source mobile station and the destination mobile station can be written as

$$r^{(0)}(t) = \mu_\rho^{(0)}(t)s(t) + n^{(0)}(t) \tag{1}$$

where $\mu_\rho^{(0)}(t)$ models the complex channel gain of the fading channel from the source mobile station to the destination mobile station under LOS propagation conditions. The non-zero-mean complex Gaussian process $\mu_\rho^{(0)}(t)$ comprises the sum of the scattered component $\mu^{(0)}(t)$ and the LOS component $m^{(0)}(t)$ in the direct transmission link from the

http://dx.doi.org/10.5772/55333

source mobile station to the destination mobile station, i.e., $\mu_{\rho}^{(0)}(t) = \mu^{(0)}(t) + m^{(0)}(t)$. In addition, $n^{(0)}(t)$ denotes a zero-mean additive white Gaussian noise (AWGN) process with variance $N_0/2$, where N_0 is the noise power spectral density.

Similarly, we can express the signal $r^{(k)}(t)$ received from the kth diversity branch at the destination mobile station as

$$r^{(k)}(t) = \varsigma_{\rho}^{(k)}(t)s(t) + n_{\mathrm{T}}^{(k)}(t) \tag{2}$$

where $\varsigma_{\rho}^{(k)}(t)$ $(k = 1, 2, \ldots, K)$ represents the complex channel gain of the kth subchannel from the source mobile station to the destination mobile station via the kth mobile relay under LOS propagation conditions. Furthermore, $n_{\mathrm{T}}^{(k)}(t) \,\forall\, k = 1, 2, \ldots, K$ is the total noise in the link from the source mobile station to the destination mobile station via the kth mobile relay. This noise term is analyzed below.

Each fading process $\varsigma_{\rho}^{(k)}(t)$ in (2) is modeled as a weighted non-zero-mean complex double Gaussian process of the form

$$\varsigma_{\rho}^{(k)}(t) = \varsigma_{\rho_1}^{(k)}(t) + j\varsigma_{\rho_2}^{(k)}(t) = A_k\, \mu_{\rho}^{(2k-1)}(t)\mu_{\rho}^{(2k)}(t) \tag{3}$$

for $k = 1, 2, \ldots, K$. In (3), each $\mu_{\rho}^{(i)}(t)$ is a non-zero-mean complex Gaussian process. For all odd superscripts i, i.e., $i = 2k - 1 = 1, 3, \ldots, (2K - 1)$, the Gaussian process $\mu_{\rho}^{(i)}(t)$ describes the sum of the scattered component $\mu^{(i)}(t)$ and the LOS component $m^{(i)}(t)$ of the ith subchannel between the source mobile station and the kth mobile relay, i.e., $\mu_{\rho}^{(i)}(t) = \mu^{(i)}(t) + m^{(i)}(t)$. Whereas, for all even superscripts i, i.e., $i = 2k = 2, 4, \ldots, 2K$, the Gaussian process $\mu_{\rho}^{(i)}(t)$ denotes the sum of the scattered component $\mu^{(i)}(t)$ and the LOS component $m^{(i)}(t)$ of the ith subchannel between the kth mobile relay and the destination mobile station. Each scattered component $\mu^{(i)}(t)$ $(i = 0, 1, 2, \ldots, 2K)$ is modeled by a zero-mean complex Gaussian process with variance $2\sigma_i^2$. Furthermore, these Gaussian processes are supposed to be mutually independent, where the spectral properties of each process are characterized by the classical Jakes Doppler power spectral density. The corresponding LOS component $m^{(i)}(t) = \rho_i \exp\{j(2\pi f_{\rho}^{(i)} t + \theta_{\rho}^{(i)})\}$ assumes a fixed amplitude ρ_i, a constant Doppler frequency $f_{\rho}^{(i)}$, and a constant phase $\theta_{\rho}^{(i)}$.

In (3), A_k is called the relay gain of the kth relay. In order to achieve the optimum performance in a relay-based system, the selection of the relay gain A_k is of critical importance. For fixed-gain relays under NLOS propagation conditions, A_k is usually selected to be [41]

$$A_k = \frac{1}{\sqrt{E\left\{\left|\mu_{\rho\to 0}^{(2k-1)}(t)\right|^2\right\} + N_0}} \tag{4}$$

where $E\{\cdot\}$ is the expectation operator. Notice that $E\left\{\left|\mu_{\rho\to 0}^{(2k-1)}(t)\right|^2\right\} = 2\sigma_{2k-1}^2$ represents the mean power of the NLOS fading channel between the source mobile station and the kth mobile relay. Replacing $\mu_{\rho\to 0}^{(2k-1)}(t)$ by $\mu_{\rho}^{(2k-1)}(t)$ in (4) allows us to express the relay gain A_k associated with LOS propagation scenarios as

$$\begin{aligned} A_k &= \frac{1}{\sqrt{E\left\{\left|\mu_{\rho}^{(2k-1)}(t)\right|^2\right\} + N_0}} \\ &= \frac{1}{\sqrt{2\sigma_{2k-1}^2 + \rho_{2k-1}^2 + N_0}}. \end{aligned} \tag{5}$$

In practical amplify-and-forward relay systems, the total noise $n_{\mathrm{T}}^{(k)}(t)$ in the link from the source mobile station to the destination mobile station via the kth mobile relay has the following form

$$n_{\mathrm{T}}^{(k)}(t) = A_k\, \mu_{\rho}^{(2k)}(t) n^{(2k-1)}(t) + n^{(2k)}(t) \tag{6}$$

for all $k = 1, 2, \ldots, K$, where $n^{(i)}(t)$ $(i = 1, 2, \ldots, 2K)$ denotes a zero-mean AWGN process with variance $N_0/2$. It is known from the literature (see, e.g., [43] and the references therein) that the total noise $n_{\mathrm{T}}^{(k)}(t)$ can be described under NLOS propagation conditions by a zero-mean complex Gaussian process with variance $N_0 + 2\sigma_{2k}^2 N_0 / \left(2\sigma_{2k-1}^2 + N_0\right)$. It can also be shown that under LOS propagation conditions, the noise process $n_{\mathrm{T}}^{(k)}(t)$ is still a zero-mean complex Gaussian process, but the variance changes to $N_0 + \left(2\sigma_{2k}^2 + \rho_{2k}^2\right) N_0 / \left(2\sigma_{2k-1}^2 + \rho_{2k-1}^2 + N_0\right)$.

Finally, the total signal $r(t)$ at the destination mobile station, obtained after combining the signals $r^{(k)}(t)$ received from $K+1$ diversity branches, can be expressed as

$$r(t) = r^{(0)}(t) + \sum_{k=1}^{K} r^{(k)}(t) = \Xi_{\rho}(t) s(t) + N(t). \tag{7}$$

This result is valid under the assumption of perfect channel state information (CSI) at the destination mobile station. In (7), $\Xi_{\rho}(t)$ represents the fading envelope at the output of the EG combiner, which can be written as [7]

$$\Xi_{\rho}(t) = \xi(t) + \sum_{k=1}^{K} \chi_{\rho}^{(k)}(t) = \left|\mu_{\rho}^{(0)}(t)\right| + \sum_{k=1}^{K} \left|\varsigma_{\rho}^{(k)}(t)\right| \tag{8}$$

where $\xi(t)$ and $\chi_{\rho}^{(k)}(t)$ are the absolute values of $\mu_{\rho}^{(0)}(t)$ and $\varsigma_{\rho}^{(k)}(t)$, respectively. Thus, $\xi(t)$ is the classical Rice process, whereas each of the processes $\chi_{\rho}^{(k)}(t)$ can be identified as a double Rice process. In (7), $N(t)$ is the total received noise, which is given by $N(t) = n^{(0)}(t) + \sum_{k=1}^{K} n_{\mathrm{T}}^{(k)}(t)$.

http://dx.doi.org/10.5772/55333

3. Statistical analysis of EGC over M2M fading channels with LOS components

In this section, we analyze the statistical properties of EGC over M2M fading channels under LOS propagation conditions. The statistical quantities of interest include the PDF, the CDF, the LCR, and the ADF of the stochastic process $\Xi_\rho(t)$ at the output of the EG combiner.

3.1. PDF of a sum of M2M fading processes with LOS components

Under LOS propagation conditions, the received signal envelope $\Xi_\rho(t)$ at the output of the EG combiner is modeled as a sum of a classical Rice process and K independent but not necessarily identical double Rice processes. The PDF $p_{\Xi_\rho}(x)$ of this sum process can be obtained straightforwardly by solving a $(K+1)$-dimensional convolution integral. The computation of this convolution integral is however quite tedious. It can be further shown that the evaluation of the inverse Fourier transform of the characteristic function (CF) does not lead to a simple closed-form expression for the PDF $p_{\Xi_\rho}(x)$. An alternate approach is to approximate $p_\Xi(x)$ either by a simpler expression or by a series. Here, we follow the approximation approach using an orthogonal series expansion. From various options of such series, like, e.g., the Edgeworth series and the Gram-Charlier series, we apply in our analysis the Laguerre series expansion [44]. The Laguerre series provides a good approximation for PDFs that are unimodal (i.e., having a single maximum) with fast decaying tails and positive defined random variables. Furthermore, the Laguerre series is often used if the first term of the series provides a good enough statistical accuracy [44].

The PDF $p_{\Xi_\rho}(x)$ of $\Xi_\rho(t)$ can then be expressed using the Laguerre series expansion as [44]

$$p_{\Xi_\rho}(x) = \sum_{n=0}^{\infty} b_n \, e^{-x} x^{\alpha_L} L_n^{(\alpha_L)}(x) \tag{9}$$

where

$$L_n^{(\alpha_L)}(x) = e^x \frac{x^{(-\alpha_L)} d^n}{x! dx^n} \left[e^{(-x)} x^{n+\alpha_L} \right], \quad \alpha_L > -1 \tag{10}$$

denotes the Laguerre polynomial. The coefficients b_n can be given as

$$b_n = \frac{n!}{\Gamma(n+\alpha_L+1)} \int_0^{\infty} L_n^{(\alpha_L)}(x) \, p_{\Xi_\rho}(x) dx \tag{11}$$

where $x = y/\beta_L$, and $\Gamma(\cdot)$ is the gamma function [45].

Furthermore, we can obtain the parameters α_L and β_L by solving the system of equations in [44, p. 21] for $b_1 = 0$ and $b_2 = 0$, which yields

$$\alpha_L = \left[\kappa_1^2 / \kappa_2 \right] - 1, \qquad \beta_L = \kappa_2 / \kappa_1 \tag{12a,b}$$

where κ_1 corresponds to the first cumulant (i.e., the mean value) and κ_2 represents the second cumulant (i.e., the variance) of the stochastic process $\Xi_\rho(t)$. Mathematically, we can express κ_n $(n = 1, 2)$ as

$$\kappa_n = \kappa_n^{(0)} + \sum_{k=1}^{K} \kappa_n^{(k)} \tag{13}$$

where $\kappa_n^{(0)}$ are the cumulants associated with the classical Rice process $\xi(t)$. For $n = 1, 2$, the cumulants $\kappa_n^{(0)}$ are equal to [46]

$$\kappa_1^{(0)} = \sigma_0 \sqrt{\frac{\pi}{2}}\, {}_1F_1\left(-\frac{1}{2}; 1; -\rho_0^2/2\sigma_0^2\right) \tag{14a}$$

$$\kappa_2^{(0)} = 2\sigma_0^2 \left(1 + \rho_0^2/2\sigma_0^2\right) - \frac{\pi}{2}\sigma_0^2 \left[{}_1F_1\left(-\frac{1}{2}; 1; -\rho_0^2/2\sigma_0^2\right)\right]^2. \tag{14b}$$

In (13), $\kappa_n^{(k)}$ $(k = 1, 2, \ldots, K)$ denote the cumulants of the double Rice process $\chi_\rho^{(k)}(t)$. The mean value and the variance of $\chi_\rho^{(k)}(t)$ are as follows [37]

$$\kappa_1^{(k)} = A_k \sigma_{2k-1} \sigma_{2k} \frac{\pi}{2}\, {}_1F_1\left(-\frac{1}{2}; 1; -\rho_{2k-1}^2/2\sigma_{2k-1}^2\right)\, {}_1F_1\left(-\frac{1}{2}; 1; -\rho_{2k}^2/2\sigma_{2k}^2\right) \tag{15a}$$

$$\begin{aligned}\kappa_2^{(k)} = &- \left(A_k \sigma_{2k-1} \sigma_{2k} \frac{\pi}{2}\right)^2 \left[{}_1F_1\left(-\frac{1}{2}; 1; -\rho_{2k-1}^2/2\sigma_{2k-1}^2\right)\, {}_1F_1\left(-\frac{1}{2}; 1; -\rho_{2k}^2/2\sigma_{2k}^2\right)\right]^2 \\ &+ A_k^2 \left(2\sigma_{2k-1}^2 + \rho_{2k-1}^2\right)\left(2\sigma_{2k}^2 + \rho_{2k}^2\right).\end{aligned} \tag{15b}$$

It is imperative to stress that here $\kappa_n^{(k)}$ is computed using the expression for A_k given in (5). In (14a) – (15b), ${}_1F_1(\cdot;\cdot;\cdot)$ is the hypergeometric function [45], which can be expanded as

$${}_1F_1\left(-\frac{1}{2}; 1; -\frac{\rho_i^2}{2\sigma_i^2}\right) = e^{-\frac{\rho_i^2}{4\sigma_i^2}} \left[\left(1 + \frac{\rho_i^2}{2\sigma_i^2}\right) I_0\left(\frac{\rho_i^2}{4\sigma_i^2}\right) + \frac{\rho_i^2}{2\sigma_i^2} I_1\left(\frac{\rho_i^2}{4\sigma_i^2}\right)\right] \tag{16}$$

where $I_n(\cdot)$ is the nth order modified Bessel function of the first kind [45].

The evaluation of κ_n in (13) is rather straightforward once we have $\kappa_n^{(0)}$ and $\kappa_n^{(k)}$ $(n = 1, 2)$ characterizing $\xi(t)$ and $\chi_\rho^{(k)}(t)$, respectively. Given κ_n, the quantities α_L and β_L can easily be computed using (12a,b). Substituting α_L and β_L in the Laguerre series expansion leads to the exact solution for the PDF $p_{\Xi_\rho}(x)$. Note that the first term of the Laguerre series can be identified as the gamma distribution $p_\Gamma(x)$ [44]. This makes it possible for us to approximate the PDF $p_{\Xi_\rho}(x)$ of $\Xi_\rho(t)$ to the gamma distribution $p_\Gamma(x)$, i.e.,

$$p_{\Xi_\rho}(x) \approx p_\Gamma(x) = \frac{x^{\alpha_L}}{\beta_L^{(\alpha_L+1)}\Gamma(\alpha_L + 1)} e^{-\frac{x}{\beta_L}}. \tag{17}$$

http://dx.doi.org/10.5772/55333

The motivation behind deriving an expression for the PDF $p_{\Xi_\rho}(x)$ of $\Xi_\rho(t)$ is that it can be utilized with ease in the link level performance analysis of dual-hop cooperative networks with EGC. This performance analysis, which results in simple closed-form expressions, is presented in Section 4.

3.2. CDF of a sum of M2M fading processes with LOS components

The probability that $\Xi_\rho(t)$ remains below the threshold level r defines the CDF $F_{\Xi_{\rho-}}(r)$ of $\Xi_\rho(t)$ [47]. After substituting (17) in $F_{\Xi_{\rho-}}(r) = 1 - \int_r^\infty p_{\Xi_\rho}(x)dx$ and solving the integral over x using [45, Eq. (3.381-3)], we can write the CDF $F_{\Xi_{\rho-}}(r)$ in closed form as

$$F_{\Xi_{\rho-}}(r) \approx 1 - \frac{1}{\Gamma(\alpha_L + 1)}\Gamma(\alpha_L, \frac{r}{\beta_L}) \tag{18}$$

where $\Gamma(\cdot,\cdot)$ is the upper incomplete gamma function [45].

3.3. LCR of a sum of M2M fading processes with LOS components

The LCR $N_{\Xi_\rho}(r)$ of $\Xi_\rho(t)$ is a measure to describe the average number of times the stochastic process $\Xi_\rho(t)$ crosses a particular threshold level r from up to down (or from down to up) in a second. The LCR $N_{\Xi_\rho}(r)$ can be computed using the formula [48]

$$N_{\Xi_\rho}(r) = \int_0^\infty \dot{x}\, p_{\Xi_\rho\dot{\Xi}_\rho}(r,\dot{x})d\dot{x} \tag{19}$$

where $p_{\Xi_\rho\dot{\Xi}_\rho}(r,\dot{x})$ is the joint PDF of the stochastic process $\Xi_\rho(t)$ and its corresponding time derivative $\dot{\Xi}_\rho(t)$ at the same time t. Throughout this paper, the overdot represents the time derivative. The task at hand is to find the joint PDF $p_{\Xi_\rho\dot{\Xi}_\rho}(r,\dot{x})$. In Section 3.1, we have shown that the PDF $p_\Xi(x)$ of $\Xi(t)$ can efficiently be approximated by the gamma distribution $p_\Gamma(x)$. Based on this fact, we assume that the joint PDF $p_{\Xi\dot{\Xi}}(r,\dot{x})$ is approximately equal to the joint PDF $p_{\Gamma\dot{\Gamma}}(r,\dot{x})$ of a gamma process and its corresponding time derivative at the same time t, i.e.,

$$p_{\Xi_\rho\dot{\Xi}_\rho}(r,\dot{x}) \approx p_{\Gamma\dot{\Gamma}}(r,\dot{x})\,. \tag{20}$$

A gamma distributed process is equivalent to a squared Nakagami-m distributed process [49]. Thus, applying the concept of transformation of random variables [47, p. 244], we can express the joint PDF $p_{\Gamma\dot{\Gamma}}(x,\dot{x})$ in terms of the joint PDF $p_{N\dot{N}}(y,\dot{y})$ of a Nakagami-m distributed process and its corresponding time derivative at the same time t as

$$p_{\Gamma\dot{\Gamma}}(x,\dot{x}) = \frac{1}{4x}p_{N\dot{N}}\left(\sqrt{x}, \frac{\dot{x}}{2\sqrt{x}}\right)\,. \tag{21}$$

After substituting $p_{N\dot{N}}(y,\dot{y})$ as given in [50, Eq. (13)] in (21), the joint PDF $p_{\Gamma\dot{\Gamma}}(x,\dot{x})$ can be written as

$$p_{\Gamma\dot{\Gamma}}(x,\dot{x}) = \frac{1}{2\sqrt{2\pi x}\dot{\sigma}} \frac{x^{(m-1)}}{(\Omega/m)^m \Gamma(m)} e^{-\frac{x}{(\Omega/m)} - \frac{\dot{x}^2}{8\dot{\sigma}^2 x}} \tag{22}$$

where m, Ω, and $\dot{\sigma}$ are the parameters associated with the Nakagami-m distribution. The result in (22) can be expressed in terms of the parameters of the gamma distribution, i.e., α_L and β_L, as

$$p_{\Gamma\dot{\Gamma}}(x,\dot{x}) = \frac{1}{2\sqrt{2\pi\beta x}} \frac{x^{\alpha_L}}{\beta_L^{(\alpha_L+1)}\Gamma(\alpha_L+1)} e^{-\frac{x}{\beta_L} - \frac{\dot{x}^2}{8\beta x}} \tag{23}$$

For a classical Rayleigh fading channel, β is the negative curvature of the autocorrelation of the inphase and quadrature components of the underlying gaussian processes [46]. Keeping the expression of β for classical Rayleigh channels in mind, we can intuitively equate β with $\pi^2(\kappa_n^{(0)}/\kappa_n^{(0)})(f_{\mathrm{S_{max}}}^2 + f_{\mathrm{D_{max}}}^2) + \pi^2(\sum_{k=1}^{K}\kappa_2^{(k)}/\sum_{k=1}^{K}\kappa_1^{(k)})(f_{\mathrm{S_{max}}}^2 + 2f_{\mathrm{R_{max}}}^2 + f_{\mathrm{D_{max}}}^2)$ here. The quantities $f_{\mathrm{S_{max}}}$ and $f_{\mathrm{D_{max}}}$ represent the maximum Doppler frequencies caused by the motion of the source mobile station and the destination mobile station, respectively. For simplicity reasons, the maximum Doppler frequencies caused by the motion of mobile relays are assumed to be equal such that $f_{\mathrm{R_{max}}}^{(1)} = f_{\mathrm{R_{max}}}^{(2)} = \cdots = f_{\mathrm{R_{max}}}^{(K)} = f_{\mathrm{R_{max}}}$.

Finally, substituting $p_{\Xi_\rho\dot{\Xi}_\rho}(r,\dot{x})$ in (19) and solving the integral over $\dot{x}$ using [45, Eq. (3.326-2)], we reach a closed-form solution for the LCR $N_{\Xi_\rho}(r)$, i.e.,

$$N_{\Xi_\rho}(r) \approx \int_0^\infty \dot{x}\, p_{\Gamma\dot{\Gamma}}(r,\dot{x})d\dot{x} = \sqrt{\frac{2r\beta}{\pi}} \frac{r^{\alpha_L} e^{-\frac{r}{\beta_L}}}{\beta_L^{(\alpha_L+1)}\Gamma(\alpha_L+1)} = \sqrt{\frac{2r\beta}{\pi}} p_{\Xi_\rho}(r) \tag{24}$$

which shows that the LCR $N_{\Xi_\rho}(r)$ is approximately proportional to the PDF $p_{\Xi_\rho}(r)$ of $\Xi_\rho(t)$.

3.4. ADF of a sum of M2M fading processes with LOS components

The ADF $T_{\Xi_{\rho-}}(r)$ of $\Xi_\rho(t)$ is the expected value of the time intervals over which the stochastic process $\Xi_\rho(t)$ remains below a certain threshold level r. Mathematically, the ADF $T_{\Xi_{\rho-}}(r)$ is defined as the ratio of the CDF $F_{\Xi_{\rho-}}(r)$ and the LCR $N_{\Xi_\rho}(r)$ of $\Xi_\rho(t)$ [7], i.e.,

$$T_{\Xi_{\rho-}}(r) = \frac{F_{\Xi_{\rho-}}(r)}{N_{\Xi_\rho}(r)}\,. \tag{25}$$

By substituting (18) and (24) in (25), we can easily obtain an approximate solution for the ADF $T_{\Xi_{\rho-}}(r)$.

The significance of studying the LCR $N_{\Xi_\rho}(r)$ and the ADF $T_{\Xi_{\rho-}}(r)$ of $\Xi_\rho(t)$ lies in the fact that they provide an insight into the rate of fading of the stochastic process $\Xi_\rho(t)$. The knowledge about the rate of fading is essential for both the design as well as the optimization of coding and interleaving schemes to combat M2M fading in the relay links in cooperative networks.

http://dx.doi.org/10.5772/55333

4. Performance analysis in M2M fading channels with LOS components and EGC

This section is dedicated to the system's performance analysis in M2M fading channels with EGC under LOS propagation conditions. The performance evaluation measures of interest include the PDF as well as the moments of the SNR, AOF, the average BEP, and the outage probability.

4.1. Analysis of the SNR

4.1.1. Derivation of the instantaneous SNR expression

We computed the total received signal envelope at the output of the EG combiner $\Xi_\rho(t)$ and the total received noise $N(t)$ in Section 2. Using these results, we can now express the instantaneous SNR per bit $\gamma_{\text{EGC}}(t)$ at the output of the EG combiner as [51, 52]

$$\gamma_{\text{EGC}}(t) = \frac{\Xi_\rho^2(t)}{E\{N^2(t)\}} E_b \tag{26}$$

where E_b is the energy (in joules) per bit and $E\{N^2(t)\}$ is the variance of the noise term at the output of the matched filter. Evaluating $E\{N^2(t)\}$ leads us to

$$\begin{aligned} E\{N^2(t)\} &= E\left\{\left(n^{(0)}(t) + \sum_{k=1}^{K} n_{\text{T}}^{(k)}(t)\right)^2\right\} \\ &= (K+1)N_0 + \sum_{k=1}^{K} \frac{2\sigma_{2k}^2 + \rho_{2k}^2}{2\sigma_{2k-1}^2 + \rho_{2k-1}^2 + N_0} N_0 \,. \end{aligned} \tag{27}$$

4.1.2. PDF of the SNR

The PDF $p_{\gamma_{\text{EGC}}}(z)$ of $\gamma_{\text{EGC}}(t)$ can be obtained using the relation

$$p_{\gamma_{\text{EGC}}}(z) = \frac{1}{(E_b/E\{N^2(t)\})}\, p_{\Xi_\rho^2}\left(\frac{z}{E_b/E\{N^2(t)\}}\right) \tag{28}$$

where $p_{\Xi_\rho^2}(z)$ is the squared received signal envelope $\Xi_\rho^2(t)$ at the output of the EG combiner, which can be obtained by a simple transformation of the random variables [47, p. 244] as follows

$$\begin{aligned} p_{\Xi_\rho^2}(z) &= \frac{1}{2\sqrt{z}} p_{\Xi_\rho}(\sqrt{z}) \\ &\approx \frac{1}{2\beta_L^{(\alpha_L+1)}\Gamma(\alpha_L+1)} z^{(\frac{\alpha_L-1}{2})} e^{-\frac{\sqrt{z}}{\beta_L}}, \quad z \geq 0 \,. \end{aligned} \tag{29}$$

The substitution of (29) in (28) leads us to the approximation for the PDF $p_{\gamma_{\mathrm{EGC}}}(z)$ of $\gamma_{\mathrm{EGC}}(t)$ in the following closed form expression

$$p_{\gamma_{\mathrm{EGC}}}(z) \approx \frac{1}{2(E_b/E\{N^2(t)\})^{\left(\frac{\alpha_L+1}{2}\right)}} \frac{z^{\left(\frac{\alpha_L-1}{2}\right)}}{\beta_L^{(\alpha_L+1)}\Gamma(\alpha_L+1)} e^{-\frac{\sqrt{z}}{\beta_L\sqrt{E_b/E\{N^2(t)\}}}}. \tag{30}$$

4.1.3. Moments of the SNR

Substituting (30) in $m_{\gamma_{\mathrm{EGC}}}^{(n)} = \int_{-\infty}^{\infty} z^n \, p_{\gamma_{\mathrm{EGC}}}(z)dz$ and solving the integral over z using [45, Eq. (3.478-1)] allows us to express approximately the nth moment of the SNR $\gamma_{\mathrm{EGC}}(t)$ in closed form as

$$m_{\gamma_{\mathrm{EGC}}}^{(n)} \approx \beta_L^{2n} \left(\frac{E_b}{E\{N^2(t)\}}\right)^n \frac{\Gamma(\alpha_L+2n+1)}{\Gamma(\alpha_L+1)}. \tag{31}$$

4.1.4. Amount of Fading

The AOF is defined as the ratio of the variance $\sigma_{\gamma_{\mathrm{EGC}}}^2$ and the squared mean value $m_{\gamma_{\mathrm{EGC}}}^{(1)}$ of the SNR $\gamma_{\mathrm{EGC}}(t)$, i.e., [26, 53]

$$\mathrm{AOF} = \frac{\sigma_{\gamma_{\mathrm{EGC}}}^2}{\left(m_{\gamma_{\mathrm{EGC}}}^{(1)}\right)^2} = \frac{m_{\gamma_{\mathrm{EGC}}}^{(2)} - \left(m_{\gamma_{\mathrm{EGC}}}^{(1)}\right)^2}{\left(m_{\gamma_{\mathrm{EGC}}}^{(1)}\right)^2}. \tag{32}$$

Computing the first two moments of $\gamma_{\mathrm{EGC}}(t)$ using (31) and substituting the results in (32) yields the following closed-form approximation for the AOF

$$\mathrm{AOF} \approx \left(\alpha_L^2 + 7\alpha_L + 12\right) \beta_L^2 \Gamma(\alpha_L+1) - 1. \tag{33}$$

4.2. Average BEP

By way of example, we focus on the average BEP P_b of M-ary PSK modulation schemes. The average BEP P_b over the fading channel statistics at the output of the EG combiner can be obtained using the formula [51]

$$P_b = \int_0^{\infty} p_{\Xi_\rho}(x) P_{b|\Xi_\rho}(x)dx \tag{34}$$

where $P_{b|\Xi_\rho}(x)$ is the BEP of M-ary PSK modulation schemes conditioned on the fading amplitudes $\{x_k\}_{k=0}^K$, and $x = \sum_{k=0}^K x_k$. Here, the fading amplitude x_0 follows the classical

http://dx.doi.org/10.5772/55333

Rice distribution. Furthermore, the fading amplitudes $\{x_k\}_{k=1}^{K}$ are characterized by the double Rice distribution.

The conditional BEP $P_{b|\Xi_\rho}(x)$ of M-ary PSK modulation schemes can be approximated as [54]

$$\begin{aligned} P_{b|\Xi_\rho}(x) &\approx \frac{a}{\log_2 M} Q\left(\sqrt{2g \log_2 M \gamma_{\text{EGC}}(x)}\right) \\ &\approx \frac{a}{\log_2 M} Q\left(\sqrt{\frac{2g \log_2 M E_b}{E\{N^2(t)\}} x^2}\right) \end{aligned} \tag{35}$$

where $M = 2^b$ with b as the number of bits per symbol, and $Q(\cdot)$ is the error function [45]. The parameter a equals 1 or 2 for M-ary PSK modulation schemes when $M = 2$ or $M > 2$, respectively, whereas for all M-ary PSK modulation schemes $g = \sin^2(\pi/M)$ [39].

Substituting (17) and (35) in (34) leads to the approximate solution for the average BEP P_b in the form

$$P_b \approx \frac{a}{\log_2 M} \frac{1}{\beta_L^{(\alpha_L+1)} \Gamma(\alpha_L+1)} \int_0^\infty x^{\alpha_L} e^{-\frac{x}{\beta_L}} Q\left(\sqrt{\frac{2g \log_2 M E_b}{E\{N^2(t)\}} x^2}\right) dx\,. \tag{36}$$

4.3. Outage Probability

The outage probability $P_{\text{out}}(\gamma_{th})$ is defined as the probability that the SNR $\gamma_{\text{EGC}}(t)$ at the output of the EG combiner falls below a certain threshold level γ_{th}. Substituting (30) in $P_{\text{out}}(\gamma_{th}) = Pr\{\gamma_{\text{EGC}} \leq \gamma_{th}\} = 1 - \int_{\gamma_{th}}^{\infty} p_{\gamma_{\text{EGC}}}(z)dz$

$$P_{\text{out}}(\gamma_{th}) \approx 1 - \frac{1}{\Gamma(\alpha_L+1)} \Gamma\left(\alpha_L+1, \frac{\sqrt{\gamma_{th}}}{\beta_L \sqrt{E_b / E\{N^2(t)\}}}\right). \tag{37}$$

5. Numerical results

The aim of this section is to evaluate and to illustrate the derived theoretical approximations given in (17), (24), (25), (36), and (37) as well as to investigate their accuracy. The correctness of the approximated analytical results is confirmed by evaluating the statistics of the waveforms generated by utilizing the sum-of-sinusoids (SOS) method [46]. These simulation results correspond to the true (exact) results here. The waveforms $\tilde{\mu}^{(i)}(t)$ obtained from the designed SOS-based channel simulator are considered as an appropriate model for the uncorrelated Gaussian noise processes $\mu^{(i)}(t)$ making up the received signal envelope at the output of the EG combiner. The model parameters of the channel simulator have been computed by using the generalized method of exact Doppler spread (GMEDS_1) [55]. Each waveform $\tilde{\mu}^{(i)}(t)$ was generated with $\text{N}_l^{(i)} = 14$ for $i = 0, 1, 2, \ldots, 2K$ and $l = 1, 2$, where

$N_l^{(i)}$ is the number of sinusoids chosen to simulate the inphase ($l = 1$) and quadrature ($l = 2$) components of $\tilde{\mu}^{(i)}(t)$. It is widely acknowledged that the distribution of the absolute value $\left|\tilde{\mu}^{(i)}(t)\right|$ of the simulated waveforms closely approximates the Rayleigh distribution if $N_l^{(i)} \geq 7 (l = 1, 2)$ [46]. Thus, by selecting $N_l^{(i)} = 14$, we ensure that the waveforms $\tilde{\mu}^{(i)}(t)$ have the required Gaussian distribution. The variance of the inphase and quadrature component of $\mu^{(i)}(t)$ ($\tilde{\mu}^{(i)}(t)$) is equal to $\sigma_i^2 = 1 \forall\ i = 0, 1, 2, \ldots, 2K$, unless stated otherwise. The maximum Doppler frequencies caused by the motion of the source mobile station, K mobile relays, and the destination mobile station, denoted by $f_{S_{max}}$, $f_{R_{max}}$, and $f_{D_{max}}$, were set to 91 Hz, 125 Hz, and 110 Hz, respectively. The total number of symbols generated for a reliable evaluation of the BEP curves was 10^7.

In this section, we have attempted to highlight the influence of a LOS component on the statistics of the received signal envelope at the output of the EG combiner and the system's overall performance. This is done by considering three propagation scenarios called the full-LOS, the partial-LOS, and the NLOS scenario, denoted by $LOS_{K,K}$, $LOS_{K,0}$ ($LOS_{0,K}$), and $LOS_{0,0}$, respectively. Here, K corresponds to the number of mobile relays in the network. In the full LOS scenario, we have LOS components in the direct link as well as all the transmission links between the source mobile station and the destination mobile station via K mobile relays. The scenario in which LOS components are present in only a few links from the source mobile station to the destination mobile station via K mobile relays is referred to as the partial-LOS scenario. When LOS components do not exist in any of the transmission links, we have the NLOS scenario. Whenever, there exists a LOS component in any of the transmission links, its amplitude ρ_i is taken to be unity. It is necessary to keep in mind that there is a direct link between the source mobile station and the destination mobile station, in addition to the links via K mobile relays. Therefore, the total number of diversity branches available is $K + 1$. The presented results in Figs. 2–8 display a good fit of the approximated analytical and the exact simulation results.

Figure 2 demonstrates the theoretical approximation for the PDF $p_{\Xi_\rho}(x)$ of $\Xi_\rho(t)$ described in (17). This figure illustrates the PDF $p_{\Xi_\rho}(x)$ under full-LOS, partial-LOS, and NLOS propagation conditions considering a different number of mobile relays K. It is quite obvious from the figure that for any value of K, the presence of LOS components increases both the mean value and the variance of $\Xi_\rho(t)$. Furthermore, for the $LOS_{K,K}$ scenario if $K = 1$, the PDF $p_{\Xi_\rho}(x)$ maps to the double Rice distribution as $\sigma_0^2 \to 0$, whereas $p_{\Xi_\rho}(x)$ reduces to the double Rayleigh distribution for the $LOS_{0,0}$ scenario. Another important result is that the PDF $p_{\Xi_\rho}(x)$ of $\Xi_\rho(t)$ tends to a Gaussian distribution if K increases. This observation is in accordance with the central limit theorem [47]. A close agreement between the approximated theoretical and the exact simulation results confirms the correctness of our approximation.

The LCR $N_{\Xi_\rho}(r)$ of $\Xi_\rho(t)$ described by (24) is evaluated along with the exact simulation results in Fig. 3. This figure presents the LCR $N_{\Xi_\rho}(r)$ of $\Xi_\rho(t)$ corresponding to the $LOS_{K,K}$, $LOS_{K,0}$ ($LOS_{0,K}$), and $LOS_{0,0}$ scenarios considering a different number of mobile relays K in the system. It can be observed that in general, for any value of K, at low signal levels r, the LOS components facilitate in decreasing the LCR $N_{\Xi_\rho}(r)$. However, at high signal levels r, the presence of LOS components contributes towards an increase in $N_{\Xi_\rho}(r)$. These results also illustrate that for all the three considered propagation scenarios, at any signal level r, (24) closely approximates the exact simulation results if $K > 1$. This is in contrast to the case

http://dx.doi.org/10.5772/55333

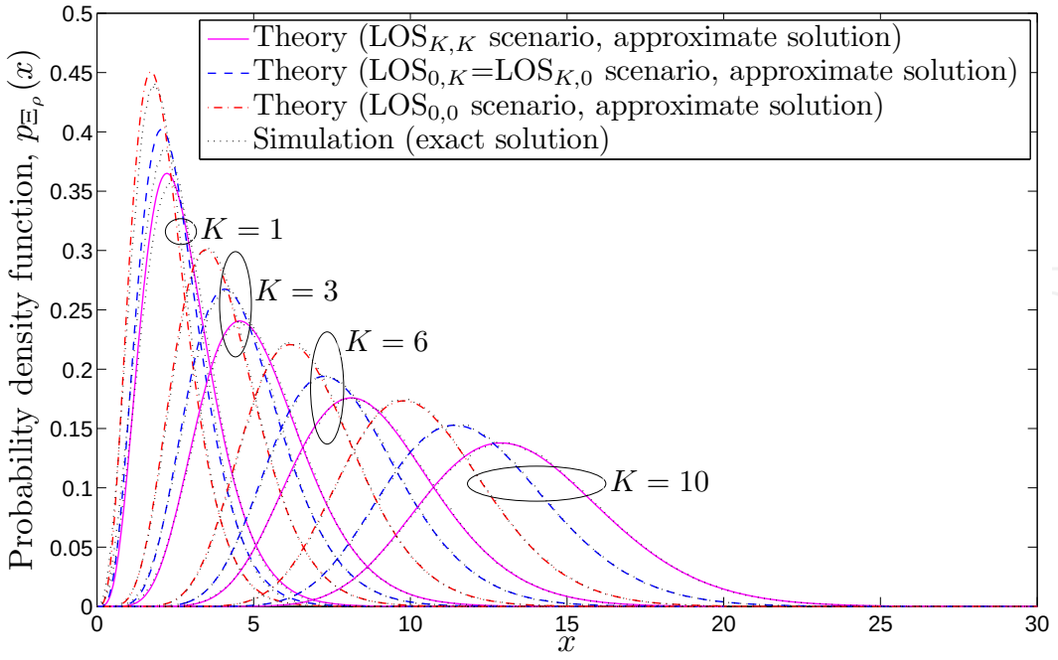


Figure 2. The PDF $p_{\Xi_\rho}(x)$ of the received signal envelope $\Xi_\rho(t)$ at the output of the EG combiner for $K+1$ diversity branches under different propagation conditions.

if $K = 1$, where (24) holds only for high values of r. We can further deduce from these results that by increasing K, $N_{\Xi_\rho}(r)$ reduces (increases) at low (high) values of r. It is also worth noticing that at high values of r, for the LOS$_{K,K}$ scenario if $K = 1$, as $\sigma_0^2 \to 0$, (24) provides us with a very close approximation to the exact LCR of a double Rice process given in [37], whereas it approximates well to the exact LCR of a double Rayleigh process for the LOS$_{0,0}$ scenario [56].

Figure 4 displays the analytical approximate results of the ADF $T_{\Xi_{\rho-}}(r)$ of $\Xi_\rho(t)$ described by (25) along with the exact simulation results. These results clearly indicate that for all propagation scenarios, i.e., the LOS$_{K,K}$, LOS$_{K,0}$ (LOS$_{0,K}$), and LOS$_{0,0}$ scenarios, an increase in the number K of mobile relays results in a decrease of $T_{\Xi_{\rho-}}(r)$ at all signal levels r. It can also be observed in Fig. 4 that the presence of the LOS components in all the transmission links lowers $T_{\Xi_{\rho-}}(r)$ for all signal levels r and any number K.

The average BEP P_b of M-ary PSK modulation schemes over M2M fading channels with LOS components and EGC described by (36) is presented in Fig. 5. In this figure, a comparison of the average BEP P_b of quadrature PSK (QPSK), 8-PSK, as well as 16-PSK modulation schemes is shown by taking into account $K+1$ diversity branches for each modulation scheme. The average BEP P_b curves associated with the aforementioned modulation schemes in double Rice channels are also included in Fig. 5. Here, the average BEP P_b is evaluated for the LOS$_{K,K}$ scenario, i.e., $\rho_i = 1 \,\forall\, i = 0, 1, 2, \ldots, 2K$. For all modulation schemes, if $K = 1$, a significant enhancement in the diversity gain can be observed with the availability of just one extra transmission link. See, e.g., if the direct link from the source mobile station to the destination mobile station is not blocked by obstacles, and if there is one relay present in the system, then it is possible to attain a diversity gain of approximately 21 dB at $P_b = 10^{-3}$. Increasing the number K of mobile relays in the system, in turn increases the number of diversity branches and hence improves the performance. The provision of higher data rates is the characteristic

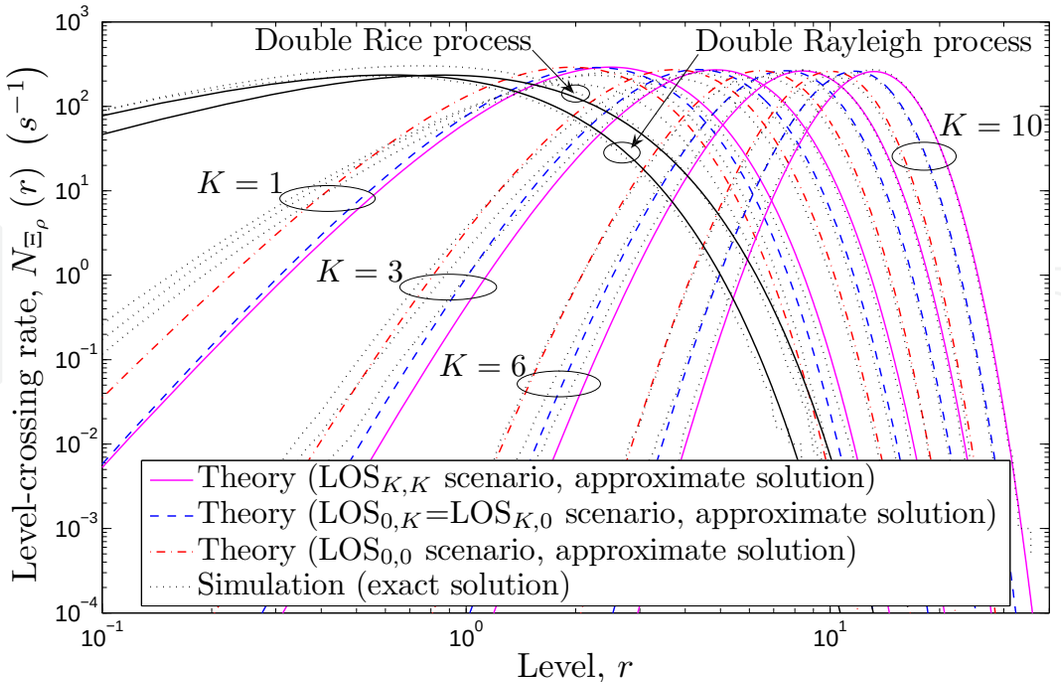


Figure 3. The LCR $N_{\Xi_\rho}(r)$ of the received signal envelope $\Xi_\rho(t)$ at the output of the EG combiner for $K+1$ diversity branches under different propagation conditions.

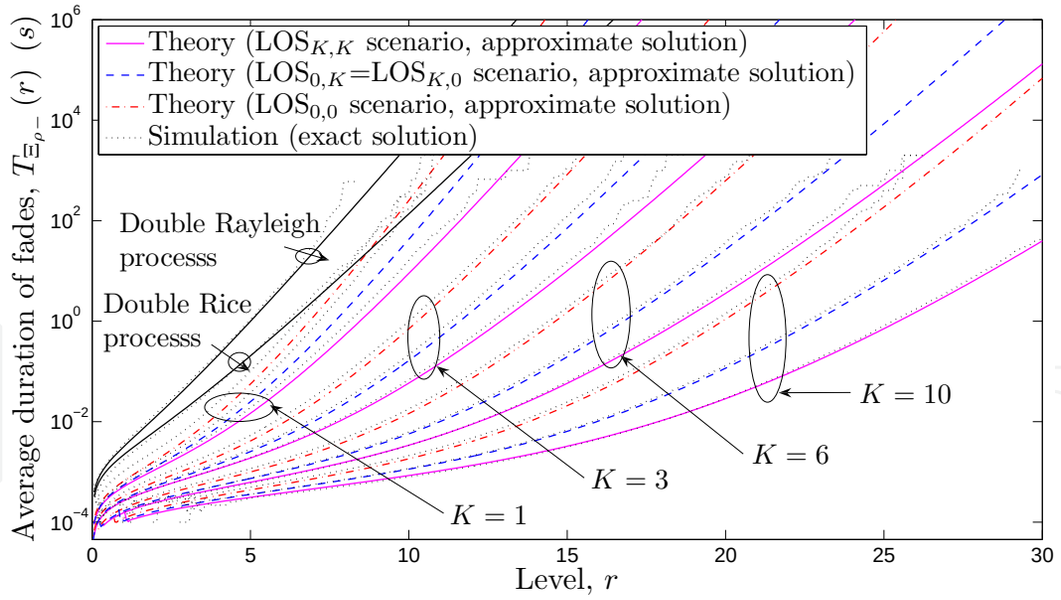


Figure 4. The ADF $T_{\Xi_{\rho-}}(r)$ of the received signal envelope $\Xi_\rho(t)$ at the output of the EG combiner for $K+1$ diversity branches under different propagation conditions.

feature of higher-order modulation schemes. These modulations are however known to be more prone to transmission errors. This sensitivity of higher-order modulations towards transmission errors is visible in Fig. 5 as the average BEP P_b curve associated with QPSK modulation shifts to the right if 8-PSK or 16-PSK modulation schemes are deployed.

http://dx.doi.org/10.5772/55333

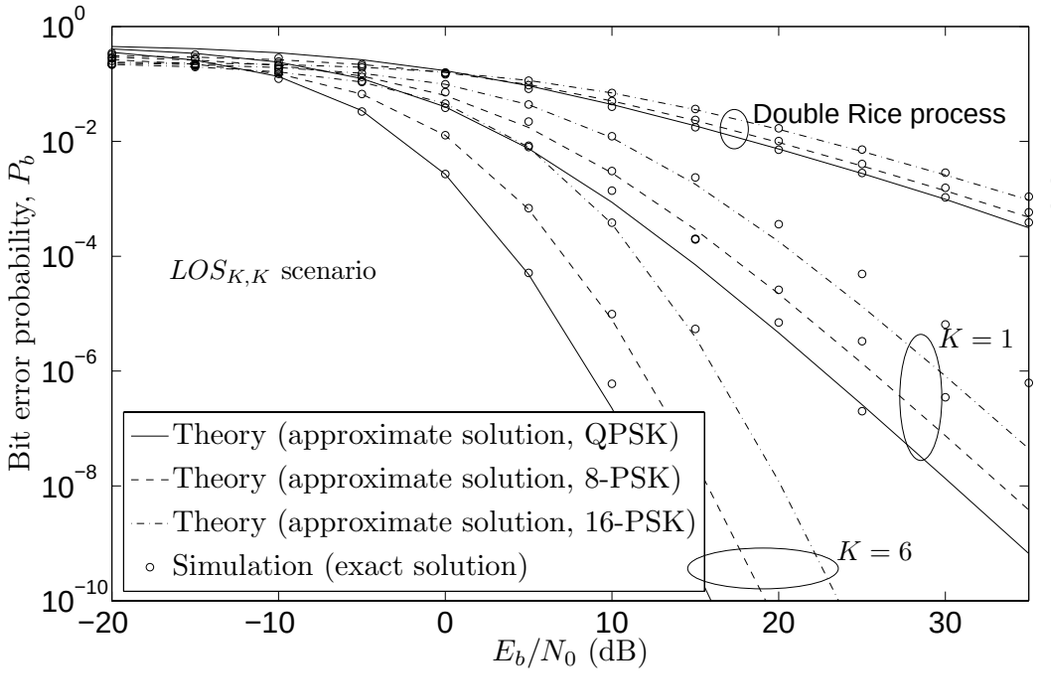


Figure 5. The average BEP P_b of M-ary PSK modulation schemes over M2M fading channels with EGC under full-LOS propagation conditions.

An EG combiner installed at the destination mobile station makes a receiver diversity system. In addition to the diversity gain, such systems offer an array gain as well [54]. The array gain in fact results from coherent combining of multiple received signals. In the context of EGC, the array gain allows the receiver diversity system in a fading channel to achieve a better performance than a system without diversity in an AWGN channel with the same average SNR [54]. Figure 6 includes the theoretical results of the average BEP P_b of QPSK under full-LOS propagation conditions (i.e., the $\text{LOS}_{K,K}$ scenario) with increasing number K of diversity branches. In the presented results, $K \geq 10$ implies that we have at least 11 diversity branches. Note that in Fig. 6, for $K \geq 10$, the dual-hop amplify-and-forward system with M2M fading channels has a lower error probability than a system in an AWGN channel with the same SNR. This improved performance is due to the array gain of the EG combiner.

Figure 7 illustrates the impact of the presence of LOS components in the relay links on the average BEP P_b of M-ary PSK modulation schemes. Keeping the number of diversity branches constant, e.g., for $K = 3$, the average BEP P_b of QPSK and 16-PSK modulation schemes is evaluated for the $\text{LOS}_{K,K}$, $\text{LOS}_{K,0}$ ($\text{LOS}_{0,K}$), and $\text{LOS}_{0,0}$ scenarios. For both QPSK and 16-PSK modulations, there is a noticeable gain in the performance if the scenario changes from $\text{LOS}_{0,0}$ to $\text{LOS}_{K,K}$. See, e.g., at $P_b = 10^{-4}$, a gain of approximately 1.5 dB is achieved when we have $\text{LOS}_{K,0}$ ($\text{LOS}_{0,K}$) compared to $\text{LOS}_{0,0}$. A further increase of approximately 1 dB in the gain can be seen if $\text{LOS}_{K,K}$ conditions are available.

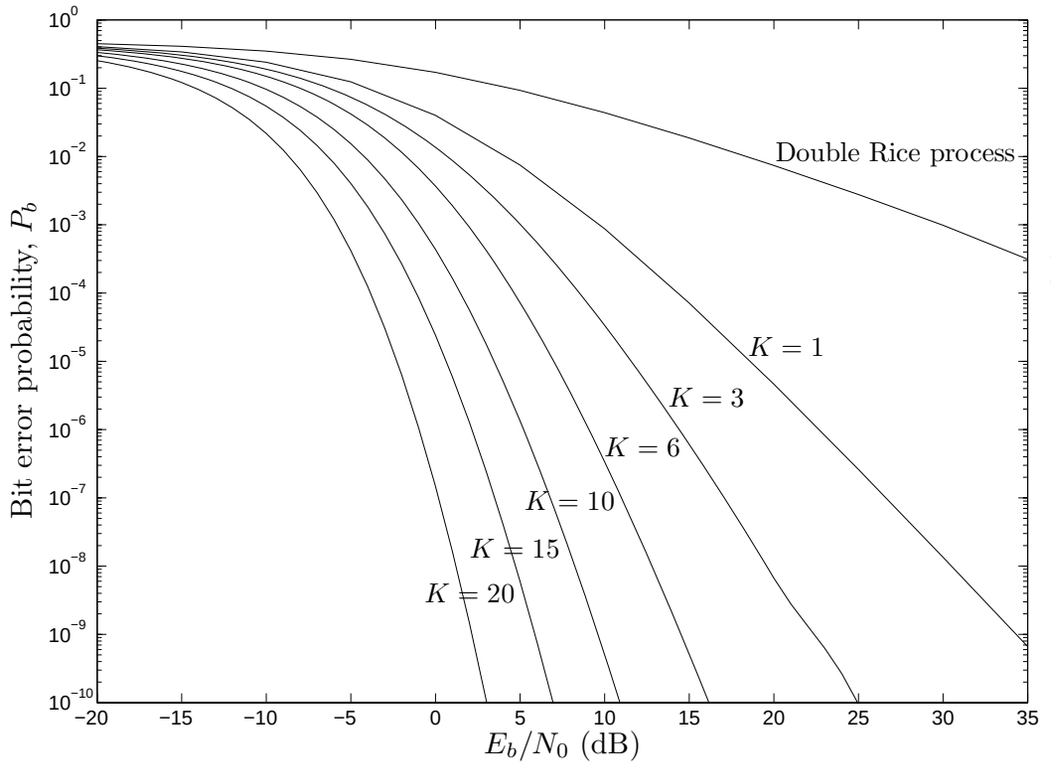


Figure 6. The average BEP P_b of QPSK modulation schemes over M2M fading channels with EGC for the $\text{LOS}_{K,K}$ scenario.

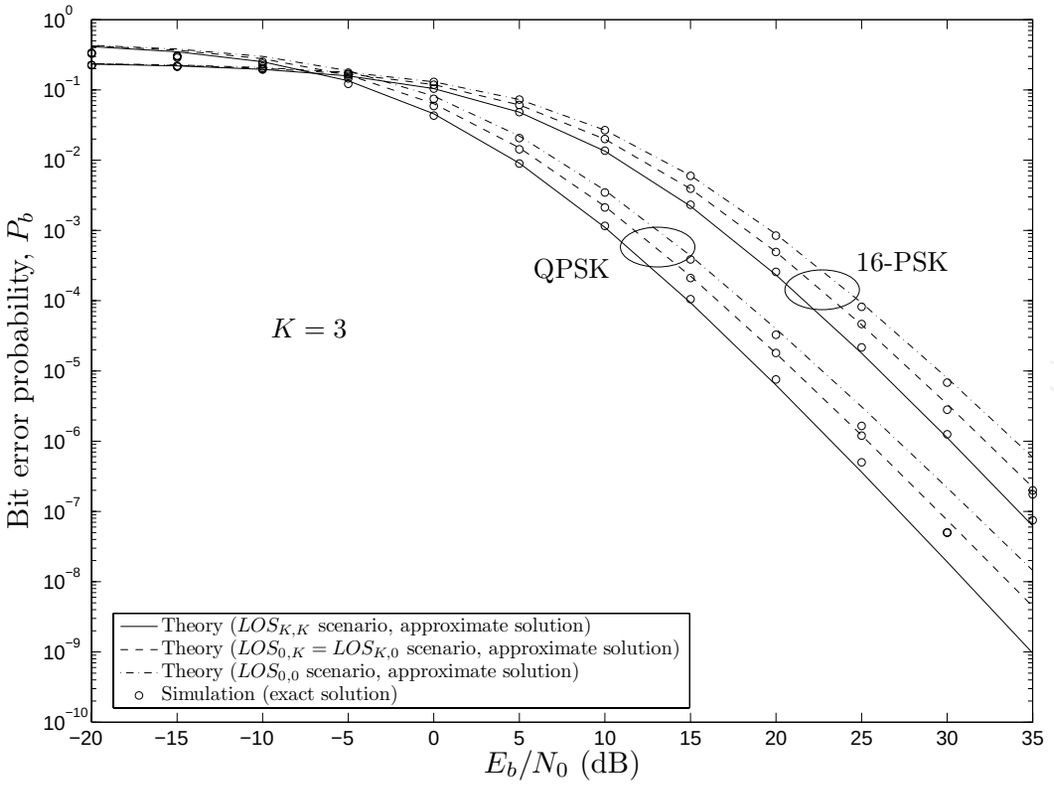


Figure 7. The average BEP P_b of M-ary PSK modulation schemes over M2M fading channels with EGC under different propagation conditions.

http://dx.doi.org/10.5772/55333

Finally, the outage probability $P_{\text{out}}(\gamma_{th})$ described by (37) is evaluated along with the exact simulation results in Fig. 8. Under full-LOS propagation conditions with the QPSK modulation scheme employed in our analysis, $P_{\text{out}}(\gamma_{th})$ is obtained for a different number of diversity branches. The presented results show a decrease in $P_{\text{out}}(\gamma_{th})$, which is due to EGC deployed at the destination mobile station, where the resulting performance advantage is the diversity gain.

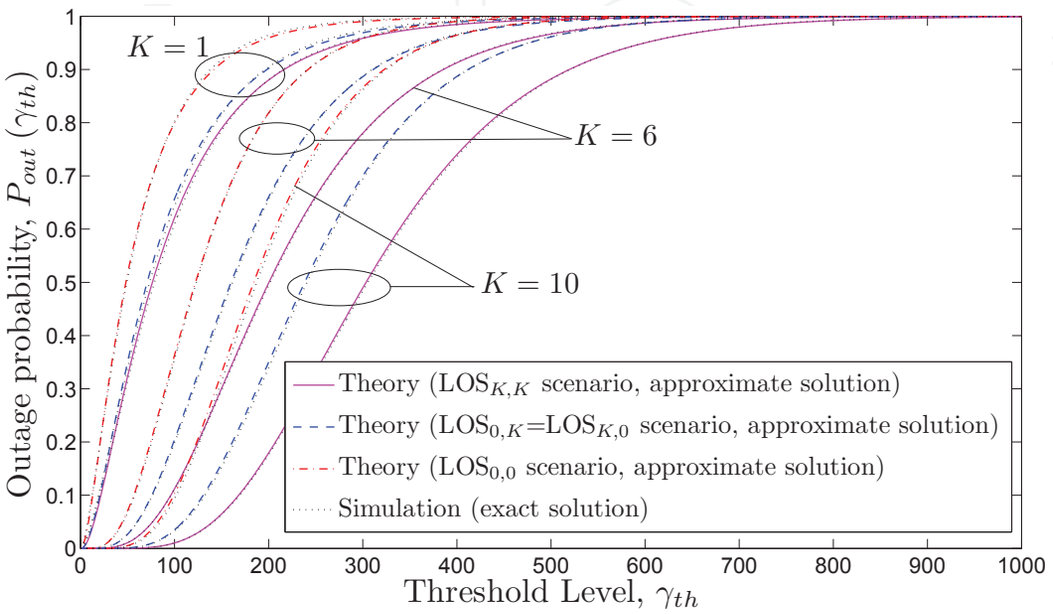


Figure 8. The outage probability $P_{\text{out}}(\gamma_{th})$ in M2M fading channels with EGC under different propagation conditions.

6. Conclusion

This article provides a profound study pertaining to the statistical properties of EGC over M2M fading channels under LOS propagation conditions in relay-based networks. In addition vital information about the performance of relay-based cooperative systems in such channels is made available. The system under investigation is a dual-hop amplify-and-forward relay communication system, where there exist K mobile relays between the source mobile station and the destination mobile station. It is further assumed that the direct link from the source mobile station to the destination mobile station is not blocked by any obstacles. Such a configuration gives rise to $K+1$ diversity branches. The signals received from the $K+1$ diversity branches are then combined at the destination mobile station to achieve the spatial diversity gain. In order to accommodate the direct link along with the unbalanced relay links, we have modeled the received signal envelope at the output of the EG combiner as a sum of a classical Rice process and K double Rice processes. Furthermore, the classical Rice process and double Rice processes are independent. Note that these double Rice processes are independent but not necessarily identically distributed.

The statistical analysis is carried out by deriving simple and closed-form analytical approximations for the channel statistics such as the PDF, CDF, LCR, and ADF. Here, the Laguerre series expansion has been employed to approximate the PDF of the sum of classical Rice and K double Rice processes. The advantage of using the Laguerre series is that this allows to approximate the PDF of the sum process by a gamma distribution with

reasonable accuracy. The CDF, LCR, and ADF of the sum process are also approximated by exploiting the properties of a gamma distributed process. Furthermore, the presented results demonstrate that the approximated theoretical results fit closely to the exact simulation results. From this fact, we can conclude that the approximation approach outlined in this study is quite useful, general, and easy to implement. In addition to studying the impact of the number of diversity branches, we have included in our discussion the influence of the existence of the LOS components in the transmission links on the statistical properties of EGC over M2M channels.

The utilization of the presented statistical analysis is then demonstrated in the performance evaluation of dual-hop multi-relay cooperative systems. In this work, the performance assessment measures of interest are the PDF as well as the moments of the SNR, AOF, the average BEP, and the outage probability. The PDF of the SNR is obtained from the previously derived PDF of the sum process by a simple transformation of random variables. Starting from the PDF of the SNR, the computation of the moments of the SNR, AOF, and the outage probability is rather straightforward.

Author details

Batool Talha and Matthias Pätzold

Department of Information and Communication Technology, Faculty of Engineering and Science, University of Agder, Grimstad, Norway

References

[1] A. Sendonaris, E. Erkip, and B. Aazhang. User cooperation diversity — Part I: System description. *IEEE Trans. Commun.*, 51(11):1927–1938, November 2003.

[2] A. Sendonaris, E. Erkip, and B. Aazhang. User cooperation diversity — Part II: Implementation aspects and performance analysis. *IEEE Trans. Commun.*, 51(11):1939–1948, November 2003.

[3] J. N. Laneman, D. N. C. Tse, and G. W. Wornell. Cooperative diversity in wireless networks: Efficient protocols and outage behavior. *IEEE Trans. Inform. Theory*, 50(12):3062–3080, December 2004.

[4] R. Pabst, B. Walke, D. Schultz, et al. Relay-based deployment concepts for wireless and mobile broadband radio. *IEEE Communications Magazine*, 42(9):80–89, September 2004.

[5] Y. Fan and J. S. Thompson. MIMO configurations for relay channels: Theory and practice. *IEEE Trans. Wireless Commun.*, 6(5):1774–1786, May 2007.

[6] M. Dohler and Y. Li. *Cooperative Communications: Hardware, Channel, and PHY*. Chichester: John Wiley & Sons, 1st edition, 2010.

[7] W. C. Jakes, editor. *Microwave Mobile Communications*. Piscataway, NJ: IEEE Press, 1994.

[8] M. D. Yacoub, C. R. C. Monterio da Silva, and J. E. V. Bautista. Second-order statistics for diversity-combining techniques in Nakagami fading channels. *IEEE Trans. Veh. Technol.*, 50(6):1464–1470, November 2001.

[9] N. C. Beaulieu and X. Dong. Level crossing rate and average fade duration of MRC and EGC diversity in Ricean fading. *IEEE Trans. Commun.*, 51(5):722–726, May 2003.

[10] P. Ivanis, D. Drajic, and B. Vucetic. The second order statistics of maximal ratio combining with unbalanced branches. *IEEE Communications Letters*, 12(7):508–510, July 2008.

[11] Q. T. Zhang. Probability of error for equal-gain combiners over Rayleigh channels: some closed-form solutions. *IEEE Trans. Commun.*, 45(3):270–273, March 1997.

[12] D. A. Zogas, G. K. Karagiannidis, and S. A. Kotsopoulos. Equal gain combining over Nakagami-*n* (Rice) and Nakagami-*q* (Hoyt) generalized fading channels. *IEEE Trans. Wireless Commun.*, 4(2):374–379, March 2005.

[13] H. Samimi and P. Azmi. An approximate analytical framework for performance analysis of equal gain combining technique over independent Nakagami, Rician and Weibull fading channels. *Wireless Personal Communications (WPC)*, 43(4):1399–1408, dec 2007. DOI 10.1007/s11277-007-9314-z.

[14] O. M. Hasna and M. S. Alouini. End-to-end performance of transmission systems with relays over Rayleigh-fading channels. *IEEE Trans. Wireless Commun.*, 2(6):1126 – 1131, November 2003.

[15] P. A. Anghel and M. Kaveh. Exact symbol error probability of a cooperative network in a Rayleigh-fading environment. *IEEE Trans. Wireless Commun.*, 3(5):1416–1421, September 2004.

[16] L. Wu, J. Lin, K. Niu, and Z. He. Performance of dual-hop transmissions with fixed gain relays over generalized-*K* fading channels. In *Proc. IEEE Int. Conf. Communications (ICC'09)*. Dresden, Germany, June 2009. DOI 10.1109/ICC.2009.5199331.

[17] T. A. Tsiftsis, G. K. Karagiannidis, and S. A. Kotsopoulos. Dual-hop wireless communications with combined gain relays. *IEE Proc. Communications*, 152(5):528 – 532, October 2005.

[18] A. Ribeiro, X. Cai, and G. B. Giannakis. Symbol error probabilities for general cooperative links. *IEEE Trans. Wireless Commun.*, 4(3):1264–1273, May 2005.

[19] Y. Li and S. Kishore. Asymptotic analysis of amplify-and-forward relaying in Nakagami fading environments. *IEEE Trans. Wireless Commun.*, 6(12):4256–4262, December 2007.

[20] W. Su, A. K. Sadek, and K. J. R. Liu. Cooperative communication protocols in wireless networks: Performance analysis and optimum power allocation. *Wireless Personal Communications (WPC)*, 44(2):181–217, January 2008.

[21] M. Di Renzo, F. Graziosi, and F. Santucci. A comprehensive framework for performance analysis of dual-hop cooperative wireless systems with fixed-gain relays over generalized fading channels. *IEEE Trans. Wireless Commun.*, 8(10):5060–5074, October 2009.

[22] H. Suraweera, G. Karagiannidis, and P. Smith. Performance analysis of the dual-hop asymmetric fading channel. *IEEE Trans. Wireless Commun.*, 8(6):2783 – 2788, June 2009.

[23] F. Xu, F. C. M. Lau, and D. W. Yue. Diversity order for amplify-and-forward dual-hop systems with fixed-gain relay under Nakagami fading channels. *IEEE Trans. Wireless Commun.*, 9(1):92 – 98, January 2010.

[24] D. B. da Costa and S. Aissa. Performance of cooperative diversity networks: Analysis of amplify-and-forward relaying under equal-gain and maximal-ratio combining. In *Proc. IEEE Int. Conf. Communications (ICC'09)*, pages 1–5. Dresden, Germany, June 2009. DOI 10.1109/ICC.2009.5199330.

[25] S. S. Ikki and M. H. Ahmed. Performance of cooperative diversity using equal gain combining (EGC) over Nakagami-*m* fading channels. *IEEE Trans. Wireless Commun.*, 8(2):557–562, February 2009.

[26] H. Q. Huynh, S. I. Husain, J. Yuan, A. Razi, and D. S. Taubman. Performance analysis of multi-branch non-regenerative relay systems with EGC in Nakagami-*m* channels. In *Proc. IEEE 70th Veh. Technol. Conf., VTC'09-Fall*, pages 1–5. Anchorage, AK, USA, September 2009. DOI 10.1109/VETECF.2009.5378710.

[27] W. R. Young. Comparison of mobile radio transmission at 150, 450, 900, and 3700 MHz. *Bell Syst. Tech. J.*, 31:1068–1085, November 1952.

[28] H. W. Nylund. Characteristics of small-area signal fading on mobile circuits in the 150 MHz band. *IEEE Trans. Veh. Technol.*, 17:24–30, October 1968.

[29] Y. Okumura, E. Ohmori, T. Kawano, and K. Fukuda. Field strength and its variability in VHF and UHF land mobile radio services. *Rev. Elec. Commun. Lab.*, 16:825–873, September/October 1968.

[30] M. Pätzold, U. Killat, and F. Laue. An extended Suzuki model for land mobile satellite channels and its statistical properties. *IEEE Trans. Veh. Technol.*, 47(2):617–630, May 1998.

[31] H. Suzuki. A statistical model for urban radio propagation. *IEEE Trans. Commun.*, 25(7):673–680, July 1977.

[32] S. Chitroub, A. Houacine, and B. Sansal. Statistical characterisation and modelling of SAR images. *Elsevier, Signal Processing*, 82(1):69–92, January 2002. DOI http://dx.doi.org/10.1016/S0165-1684(01)00158-X.

[33] P. M. Shankar. Error rates in generalized shadowed fading channels. *Wireless Personal Communications (WPC)*, 28(3):233–238, February 2004. DOI http://dx.doi.org/10.1023/B:wire.0000032253.68423.86.

http://dx.doi.org/10.5772/55333

[34] I. Z. Kovacs, P. C. F. Eggers, K. Olesen, and L. G. Petersen. Investigations of outdoor-to-indoor mobile-to-mobile radio communication channels. In *Proc. IEEE 56th Veh. Technol. Conf., VTC'02-Fall*, volume 1, pages 430–434. Vancouver BC, Canada, September 2002.

[35] M. Pätzold, B. O. Hogstad, and N. Youssef. Modeling, analysis, and simulation of MIMO mobile-to-mobile fading channels. *IEEE Trans. Wireless Commun.*, 7(2):510–520, February 2008.

[36] G. K. Karagiannidis, N. C. Sagias, and P. T. Mathiopoulos. $N*$Nakagami: A novel stochastic model for cascaded fading channels. *IEEE Trans. Commun.*, 55(8):1453–1458, August 2007.

[37] B. Talha and M. Pätzold. On the statistical properties of double Rice channels. In *Proc. 10th Int. Symp. on Wireless Personal Multimedia Communications, WPMC 2007*, pages 517âĂŞ–522. Jaipur, India, December 2007.

[38] H. Ilhan, M. Uysal, and I. Altunbas. Cooperative diversity for intervehicular communication: Performance analysis and optimization. *IEEE Trans. Veh. Technol.*, 58(7):3301 – 3310, August 2009.

[39] W. Wongtrairat and P. Supnithi. Performance of digital modulation in double Nakagami-m fading channels with MRC diversity. *IEICE Trans. Commun.*, E92-B(2):559–566, February 2009.

[40] B. Talha, M. Pätzold, and S. Primak. Performance analysis of M-ary psk modulation schemes over multiple double Rayleigh fading channels with EGC in cooperative networks. In *Proc. IEEE ICC 2010 Workshop on Vehicular Connectivity*, pages 1–6. Cape Town, South Africa, May 2010. DOI: 10.1109/ICCW.2010.5503940.

[41] R. U. Nabar, H. Bölcskei, and F. W. Kneubühler. Fading relay channels: Performance limits and space-time signal design. *IEEE J. Select. Areas Commun.*, 22(6):1099–1109, August 2004.

[42] K. Azarian, H. E. Gamal, and P. Schniter. On the achievable diversity-multiplexing tradeoff in half-duplex cooperative channels. *IEEE Trans. Inform. Theory*, 51(12):4152–4172, December 2005.

[43] Y. Wu and M. Pätzold. Parameter optimization for amplify-and-forward relaying systems with pilot symbol assisted modulation scheme. *Wireless Sensor Networks (WSN)*, 1(1):15âĂŞ–21, April 2009. DOI 10.4236/wsn.2009.11003.

[44] S. Primak, V. Kontorovich, and V. Lyandres, editors. *Stochastic Methods and their Applications to Communications: Stochastic Differential Equations Approach*. Chichester: John Wiley & Sons, 2004.

[45] I. S. Gradshteyn and I. M. Ryzhik. *Table of Integrals, Series, and Products*. New York: Academic Press, 6th edition, 2000.

[46] M. Pätzold. *Mobile Fading Channels*. Chichester: John Wiley & Sons, 2002.

[47] A. Papoulis and S. U. Pillai. *Probability, Random Variables and Stochastic Processes*. New York: McGraw-Hill, 4th edition, 2002.

[48] S. O. Rice. Mathematical analysis of random noise. *Bell Syst. Tech. J.*, 24:46–156, January 1945.

[49] M. Nakagami. The *m*-distribution: A general formula of intensity distribution of rapid fading. In W. G. Hoffman, editor, *Statistical Methods in Radio Wave Propagation*. Oxford, UK: Pergamon Press, 1960.

[50] M. D. Yacoub, J. E. V. Bautista, and L. G. de Rezende Guedes. On higher order statistics of the Nakagami-*m* distribution. *IEEE Trans. Veh. Technol.*, 48(3):790–794, May 1999.

[51] M. K. Simon and M. S. Alouini. *Digital Communications over Fading Channels*. New Jersey: John Wiley & Sons, 2nd edition, 2005.

[52] M. Schwartz, W. R. Bennett, and S. Stein. *Communication Systems and Techniques*, volume 4. New York: McGram Hill, 1966.

[53] U. Charash. Reception through Nakagami fading multipath channels with random delays. *IEEE Trans. Commun.*, 27(4):657–670, April 1979.

[54] A. Goldsmith. *Wireless Communications*. New York: Cambridge University Press, 2005.

[55] M. Pätzold, C. X. Wang, and B. O. Hogstad. Two new sum-of-sinusoids-based methods for the efficient generation of multiple uncorrelated Rayleigh fading waveforms. *IEEE Trans. Wireless Commun.*, 8(6):3122âĂŞ–3131, June 2009.

[56] C. S. Patel, G. L. Stüber, and T. G. Pratt. Statistical properties of amplify and forward relay fading channels. *IEEE Trans. Veh. Technol.*, 55(1):1–9, January 2006.

IntechOpen